

Fabrication of Low-Cost Paper-Based Microfluidic Devices by Embossing or Cut-and-Stack Methods

Martin M. Thuo,^{†,⊥,△} Ramses V. Martinez,^{†,‡,△} Wen-Jie Lan,[†] Xinyu Liu,^{†,#} Jabulani Barber,[†] Manza B. J. Atkinson,[†] Dineth Bandarage,[†] Jean-Francis Bloch,^{†,§} and George M. Whitesides^{*,†,||}

[†]Department of Chemistry and Chemical Biology, Harvard University, 12 Oxford Street, Cambridge, Massachusetts 02138, United States

[‡]Madrid Institute for Advanced Studies, IMDEA Nanoscience, Calle Faraday 9, Ciudad Universitaria de Cantoblanco, 28049 Madrid, Spain

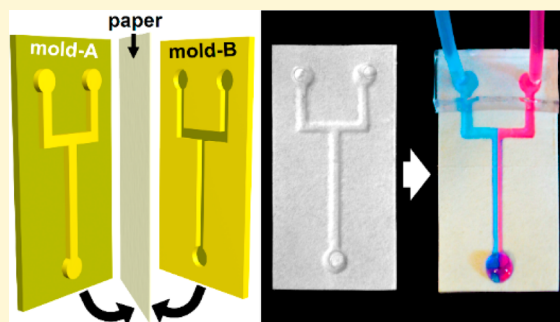
[§]Department of Papermaking Engineering - LGP2, Grenoble Institute of Technology, 461 rue de la Papeterie, BP65 - 38402 Saint Martin d'Hères, Cedex, France

^{||}Wyss Institute for Biologically Inspired Engineering, Harvard University, 60 Oxford Street, Cambridge, Massachusetts 02138, United States

[⊥]Department of Chemistry, University of Massachusetts Boston, 100 Morrissey Boulevard, Boston, Massachusetts 02125, United States

Supporting Information

ABSTRACT: This article describes the use of embossing and “cut-and-stack” methods of assembly, to generate microfluidic devices from omniphobic paper and demonstrates that fluid flowing through these devices behaves similarly to fluid in an open-channel microfluidic device. The porosity of the paper to gases allows processes not possible in devices made using PDMS or other nonporous materials. Droplet generators and phase separators, for example, could be made by embossing “T”-shaped channels on paper. Vertical stacking of embossed or cut layers of omniphobic paper generated three-dimensional systems of microchannels. The gas permeability of the paper allowed fluid in the microchannel to contact and exchange with environmental or directed gases. An aqueous stream of water containing a pH indicator, as one demonstration, changed color upon exposure to air containing HCl or NH₃ gases.



The most widely used technology for the formation of microfluidic systems—fabrication using polydimethylsiloxane (PDMS) and soft-lithography—is still too expensive and/or technically demanding for applications requiring low cost (e.g., human and veterinary medicine in resource-poor settings,¹ food testing,² or environmental monitoring³). To circumvent the issues of cost and availability, we,^{4–6} and others,^{7–9} have developed so-called “paper microfluidics” (a methodology in which fluid flow in paper is driven by capillary wetting and directed by channel boundaries of hydrophobic wax¹⁰ or polymer patterned in the paper by printing,⁷ photolithography,¹¹ or other methods¹²). Although wicking-driven paper devices are clearly attractive for their low cost, simplicity, and ability to generate 3D microfluidic systems, the cellulose fibers that partially fill the channels introduce complexity into the flow of liquids—a problem that is largely absent in open-channel PDMS-based microfluidic devices. These wicking-based devices also present a large area of potentially adsorptive surface (which may be useful or detrimental, depending on the application); the performance

of wicking devices may also be influenced by environmental factors such as humidity.

This paper is one of several introducing a new technology that, among other things, enables paper to be used as the basis for pressure-driven open-channel microfluidic systems.^{13,14} The key element in this technology is “omniphobic paper”: that is, paper whose surface has been modified by treatment with a highly fluorinated alkylsilane (and which we therefore call “R^F paper”). The static contact angle (θ_s) of water on R^F paper is high, $\theta_s = 135^\circ$ – 155° (greater than water on Teflon, $\theta_s = 120^\circ$). R^F paper is also able to resist wetting by many organic liquids: liquids with surface tensions as low as 27 mN/m (hexadecane) do not spread on R^F paper.¹⁴ Paper can be readily formed into a variety of complex 3D shapes by embossing, engraving, cutting, folding, stacking, molding, or bending. The surface modification of these paper structures by silanization (or other chemistry) enables them to be used as microfluidic

Received: May 3, 2014

Revised: June 12, 2014

devices. Combination of the shaped, surface-modified paper with other materials (polymer tapes, hydrophilic paper and thread, metal films, etc.) generates a wide range of functions and devices having low weight and low cost of materials.¹³ Shaped, R^F paper also enables new functions, because it has properties not readily encountered in conventional materials (for example, it is simultaneously inexpensive, lightweight, highly hydrophobic, highly gas permeable, easily burned, and thermally/electrically insulating).

We have described one versatile technique that involves cutting channels in cardstock paper using a programmable knife,¹³ making these engraved structures omniphobic by silanizing them using a fluorinated alkyltrichlorosilane ($R^F\text{SiCl}_3$) in the vapor phase, and sealing the channels with precut transparent tape.¹⁴ This paper describes a related method for fabricating simple open-channel microfluidic systems on Whatman #1 filter paper, based on embossing using reusable plastic molds or cutting and stacking appropriate structures into the filter paper followed by the silanization step previously mentioned. The former technique yields smaller channels and is easier to carry out; the latter is more useful for larger features and parallel production of large number of devices (by reel-to-reel embossing and processing).

Paper microfluidics, as a generic technology, would benefit from materials and systems that would preserve the advantages of paper while allowing fluids to flow in a pressure-driven open channel. These devices would find application in situations requiring the control of fluid flows afforded by open channels (for example, high-resolution capillary electrophoresis¹⁵), in applications that require manipulation of fluids containing suspended particles (such as blood, environmental slurries, multiphase suspensions, and most unprocessed biological samples),^{16,17} in analysis and/or manipulation of mixtures of compounds that would separate chromatographically in wicking-based devices,¹⁸ or in the manipulation of complex chemical mixtures.^{19,20} Open-channel microfluidic devices might also be useful in the synthesis of particles^{21,22} and in processes, such as microfluidic shear separation,²³ where the fluidic-flow properties of a liquid are of interest.

The surfaces of the cellulose fibers that make up paper have a high density of hydroxyl and acetal groups and are normally hydrophilic. Paper can be made hydrophobic by physisorption (coating the fibers or filling the voids with a hydrophobic material)^{7,10} or chemisorptions (applying reactions that modify the OH groups, such as silanization, acylation, or epoxide and thirane ring opening).¹² Of these, we have chosen silanization because (i) the reaction occurs readily at room temperature when the hydroxyl groups are exposed to vapors of a silanizing agent and (ii) there is a variety of commercially available organosilanes, with different terminal groups, that can be used to modify the surface of paper. Exposure of Whatman #1 filter paper, for example, to vapors of many perfluorinated alkylsilanes, $R^F\text{SiCl}_3$, under vacuum renders it hydrophobic (static contact angle of water, $\theta_s > 135^\circ$).¹⁴ The reaction of the hydroxyl groups of paper and alkyltrichlorosilanes, $R^F\text{SiCl}_3$, is rapid and requires no catalyst. This reagent does not react with acetal moieties and, as such, can be used for surface functionalization of paper without damaging the linkages that make up the backbone of the polymeric cellulose.

RESULTS AND DISCUSSION

Fabrication of Dies for Embossing Paper. The polymeric dies used to emboss open channels on paper were

designed using computer-aided design (CAD, Airlibre Inc.) and generated by 3D printing (StrataSys Dimension Elite) using acrylonitrile butadiene styrene (ABS) copolymer.²⁴ Paper releases readily from these ABS dies after embossing. We have used the dies over 100 with no damage or degradation in performance. Dies for embossing can also be generated via other processes such as thermoplastic casting, laser cutting, or selective etching.²⁵ The Supporting Information (Figure S1 and S2) gives detailed schematics and pictures of the embossing dies we used.

Fabrication of Open-Channel Microfluidic Devices by Embossing. We fabricated the open-channel microfluidic devices by sandwiching a sheet of paper between two dies with complementary shapes (see Figure 1a,b). Paper is compressed

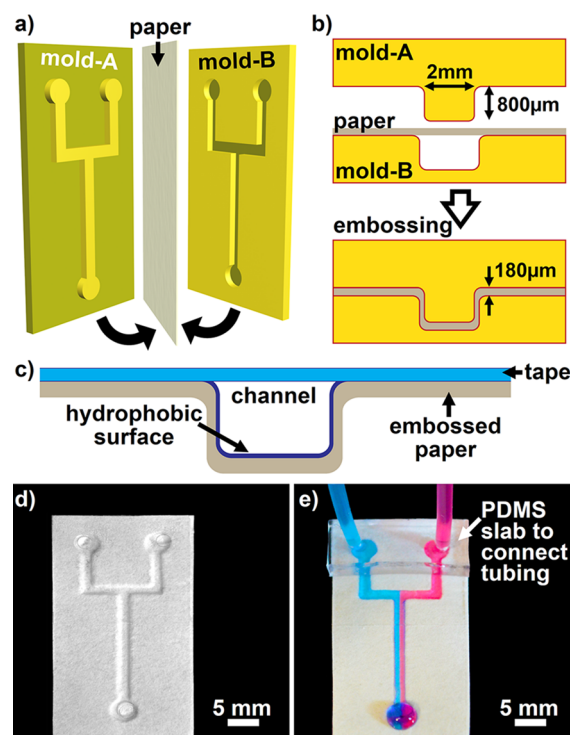


Figure 1. Laminar flow in an open-channel microfluidic device constructed by embossing channels on Whatman #1 filter paper. (a) The embossing process in which a sheet of paper is placed between two plastic molds and pressed—for dimensions, see Supporting Information Figure S1. (b) Cross-section schematic diagram of the embossing process. (c) Cross-sectional view of the finished channel with the different parts highlighted. (d) A picture of a two inlet finished device before connecting the fluid inlet tubes. The inlet tubes are supported by a small piece of PDMS elastomer and attached to the inlets using double-sided tape. (e) A picture of two streams of aqueous dye solution flowing through the microfluidic channel.

into a channel by applying pressure ($\sim 0.2 \text{ kg/cm}^2$). To increase moldability, we put a few drops of ethanol ($\sim 400 \mu\text{L}$ per device) on the paper to wet its surface and reduce its glass transition temperature.²⁶ Wetting the paper with liquid ethanol makes the paper easier to emboss with less force and avoids tearing the paper on the edges. Once embossing was finished ($\sim 2 \text{ s}$), the paper was allowed to dry for $\sim 30 \text{ s}$ in an oven at 60°C .

Silanization of Paper Devices. We made the paper devices omniphobic by silanization with $R^F\text{SiCl}_3$ (trichloro-(1H,1H,2H,2H-perfluorooctyl)silane, $\text{CF}_3(\text{CF}_2)_5(\text{CH}_2)_2\text{SiCl}_3$)

(obtained from Sigma-Aldrich and used as supplied), in a solid–vapor reaction.^{14,27} $\text{R}^{\text{F}}\text{SiCl}_3$ are relatively inexpensive: we used ~ 1 g of reagent (\$0.60) to functionalize a quantity of paper required to make >100 devices ($\sim 600\text{ cm}^2$, or $<\$0.006/\text{device}$).

Assembly of the Microfluidic Devices. We covered the channels with transparent adhesive tape (Fellowes adhesive sheet, PET/EVA/LDPE) on which inlet and outlet holes had been cut (using a laser cutter or a punch, see Figure 1c). This process for fabrication of devices is rapid (>100 devices/h) and requires no special facilities or tools. We employed this two-step method to fabricate microfluidic devices and multiple-well plates. Figure 1d,e shows a 2D microfluidic device with a channel (2 mm width, $800\text{ }\mu\text{m}$ depth) fabricated by embossing. Fluid inlet tubes were supported with 2 mm thick PDMS slabs, which were connected to the device using a double-sided adhesive layer (3M Command medium picture hanging strips, 17201, www.command.com). Figure 1e shows the laminar flow of two aqueous dye solutions at a rate of $\sim 1\text{ mL/min}$ along an embossed channel in a paper microfluidic device. The laminar flow was preserved for flow rates ranging between 0.05 and 2 mL/min without observing any leakage or delamination of the top adhesive layer. We fabricated other microfluidic designs (“T”, “+”, “U”, see Supporting Information Figures S4, S5, AND S6) and estimated the Reynolds numbers of water flowing through them to range from 45 to 1800 (at flow rates ranging from 0.05 mL/min to 2 mL/min, see Supporting Information). All devices showed laminar flow (expected for those Reynolds numbers²⁸), even when three dye solutions were introduced into the system (Supporting Information Figure S5, Movie_M1, M2, and M3).

Imaging the Channels. To understand whether embossing had a significant influence on the structure of the paper, we compared images of different parts of the devices using scanning electron microscopy (SEM) (Figure 2). Figure 2b–e shows that the fibers of the paper were stretched in the lateral walls of the channel, since these regions were where the paper was most strained during embossing. The fiber organization in the bottom of the channel is generally retained; i.e., there are no observable structural differences in fiber organization between the bottom and the nonembossed regions of the paper (Figure 2c–e). The depth profile of the embossed channel was also analyzed through contactless surface profilometry (Figure 2a). The roughness of the walls of the channel—where most stress was observed—was $\sim 22\text{ }\mu\text{m}$, while the roughness on the bottom of the channel was comparable to regions of the paper device that were not embossed ($\sim 73\text{ }\mu\text{m}$).

Three-Dimensional Microfluidic Devices. We fabricated 3D microfluidic devices on R^{F} paper using a two-layer approach (see Figure 3a). To connect the two layers of R^{F} paper, we punched holes on the top layer and through the connecting double-sided tape; these holes allowed the fluid to flow into or out of the bottom layer (Figure 3a, i to iv). To test this design, we passed solutions of dyes in water through the device (Figure 3b–d). As with the 2D microfluidic design, we observed that the fluids moved well across the channel at flow rates ranging from 0.05 mL/min to 2 mL/min (A video of this device in action is given in the Supporting Information, Movie_M4). We also ran a 3D microfluidic device using three aqueous solutions: Two on a Y-inlet leading to laminar flow, and the other solution in the cross-channel (Supporting Information Figure S7). We observed that, as the fluid moved along the channel, significant mixing was observed as a reflection of the influence of the

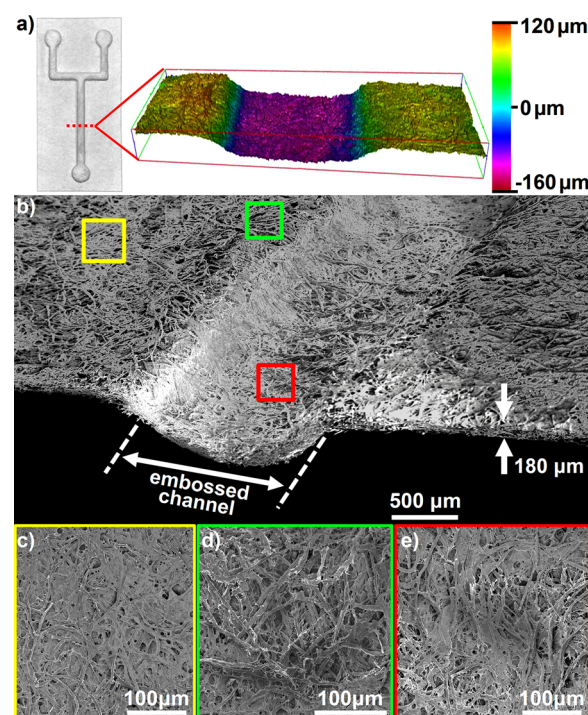


Figure 2. Physical characterization of the embossed microfluidic devices. (a) Cross-section image of the embossed channel of our microfluidic devices. The image was obtained from a ready-to-use paper device analyzed using a contactless surface profilometer. As expected, there is a sharp decline in height on the shoulders of the channel but the roughness of the bottom of the channel is comparable to that of the nonembossed regions of the paper. (b) SEM image of the embossed channel made from Whatman #1 filter paper shown in (a). (c) Highlight of a nonembossed part of the paper, distant from the embossed channel. (d) A nonembossed region on the shoulder of the embossed channel. (e) A region of the paper inside the channel.

channel architecture on the flows and eddies²⁹ (see Supporting Information Figure S6, S7, and Movie_M5).

Droplet Generators. Microfluidic droplet generators work by combining streams of immiscible liquids into one channel.^{30–32} When two streams of immiscible liquids, with low Reynolds number, meet in orthogonal channels in a T-junction (with the more rapidly flowing stream in the straight top channel), shear forces break up the more slowly flowing liquid into droplets. Embossed R^{F} paper devices are omniphobic with a rough porous surface. To generate droplets, we used a two-inlet “T” shaped device into which we introduced dyed water and dyed hexadecane (Figure 4). Neither the water nor the hexadecane wetted the omniphobic paper. Figure 4a shows a device, with inlets connected; Figure 4b shows the same device in use (Supporting Information Movie_M6). We used different flow rates to obtain monodisperse droplets of different sizes and shapes at frequencies between 0.2 and 10 Hz (Figure 4d–f). The coefficient of variation (CV) of the length of the droplets (the distance between the furthest downstream and upstream points along the interface of a fully detached plug) generated at a frequency of 1.25 Hz was 1.2%. Similar values were obtained for the experiments summarized in Figure 4g (see Supporting Information Table S1). As in other microfluidic devices,³³ droplet generation with our paper devices follows the simple scaling law (eq 1).^{34,35}

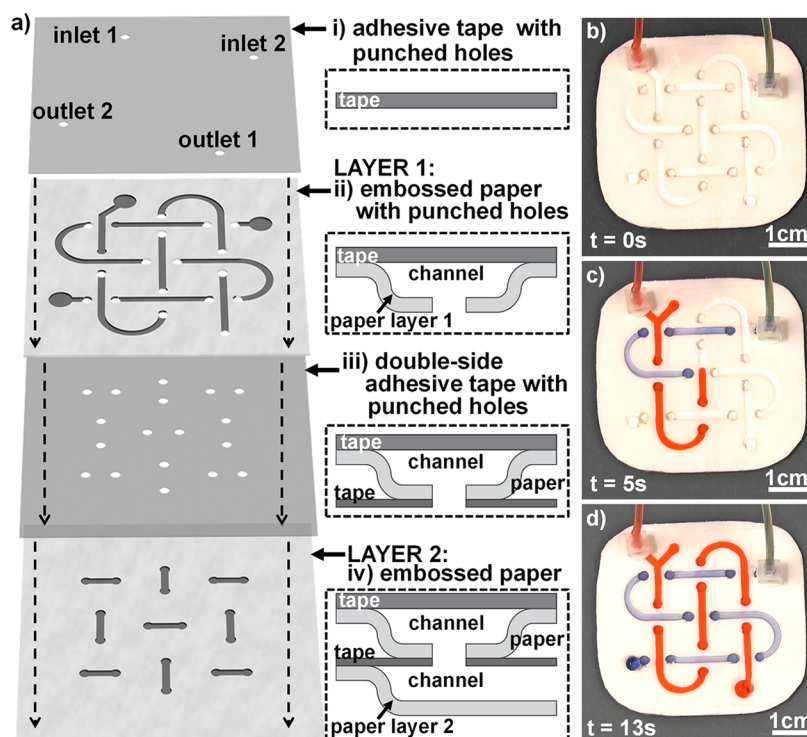


Figure 3. (a) Schematic representation of components used to fabricate the 3D embossed microfluidic devices. (i) Transparent single-sided tape (gray) with precut holes for the fluid inlets and outlet. (ii) Layer 1: top layer of channels embossed in R^F paper, with holes to allow liquid to flow under or into channels on the top paper layer. The holes are formed after embossing using a hand-held office punch or by using a laser cutter. (iii) Double-sided adhesive tape with precut holes used to connect the top and bottom channel systems (layers 1 and 2). Alignment to the two layers is critical. (iv) Layer 2: bottom layer of embossed paper channels that allow liquids to flow underneath the top layer. (b) A finished 3D microfluidic device with two inlets, attached using double-sided tape ($t = 0$ s). (c) The device during a run ($t = 5$ s, see Supporting Information Movie_M4) showing back flow at the “Y” intersection then flowing through channels in both levels. (d) After flowing ~ 2 mL of liquid through the device, two drops (blue and red) can be seen accumulating on the outlet.

$$\frac{L}{w} = 1 + \alpha \frac{Q_{\text{water}}}{Q_{\text{HD}}} \quad (1)$$

where L is the length and w is the width of the droplet, Q_{water} and Q_{HD} are the flow rates of water and hexadecane (HD), respectively, and, α is a constant that depends on the geometry of the junction. A T-inlet device generated using a knife cutter showed similar performance.¹³

Microfluidic Devices Made by Cutting and Stacking Omniphobic Paper. We have demonstrated omniphobic paper-based open-channel microfluidic devices that were realized through embossing paper. We also demonstrated that similar devices could be realized by cutting and stacking; (a) different paper labels connected with the adhesive glue already present on one side of the labels or (b) different layers of paper connected using precut double-sided tape. Figure 5a shows how to make microfluidic devices by stacking a paper label (white labels for laser printers, S-5044, www.uline.com) with the silhouette of the channel cut out on top of a nonpatterned label. We made the cut-and-stack paper devices omniphobic by silanization with R^FSiCl₃ and sealed the channel with a layer of transparent adhesive tape, as described before. In comparison to embossing, the cutting and stacking technique has six advantages: (i) No molds are needed. The cut patterns can be printed out using a regular printer or drawn with a pen and a ruler. (ii) The process has a higher success rate ($\sim 98\%$ of 60 devices tested work, as compared with $\sim 85\%$ of 240 embossed devices). (iii) Final construction consists of predictable, uniform, and tunable geometries that can be stacked on top

of others to configure a final device (Figure 5b). The patterned paper labels (or stacks of paper and tape) serve as the side walls of the channel, enabling the depth of the channel to be readily manipulated; i.e., the depth of the channel is governed by the number of paper layers that are stacked to form the channel. (iv) The flat surfaces generated in this procedure make the assembly of the devices rapid and easy, using manual procedures. (v) The adhesive layers in these devices allows for the direct insertion and sealing of the tubing into the channel, without requiring external adaptors. (Figure 5b,c). (vi) Thin microfluidic devices (~ 600 - μm thick devices were fabricated using 150 - μm thick tape and 220 - μm thick paper labels) fabricated with this technique can withstand bending and conform to curved surfaces using the adhesive of the bottom label (Figure 5c).

Figure 6 shows one type of 3D paper-based microfluidic device which has two channels crossing each other fabricated by stacking two layers of R^F paper patterned with channels on top of a layer of nonpatterned R^F paper. The channels are 2 mm wide and ~ 80 mm long. This device has two polyethylene tubes attached to the bottom layer of R^F paper to deliver gases, through the paper, into the channels (Figure 6a). Two aqueous solutions of pH indicator (yellow—Phenol Red; dark brown—Bromophenol Blue sodium salt) were introduced into the channels through the two inlets located on the top left part of the device (Figure 6b). When no gas is delivered into the channels, the color of the liquid at the outlets indicates that the device enables streams of fluid to cross one another multiple times without mixing (Figure 6c). When we deliver HCl(g) and

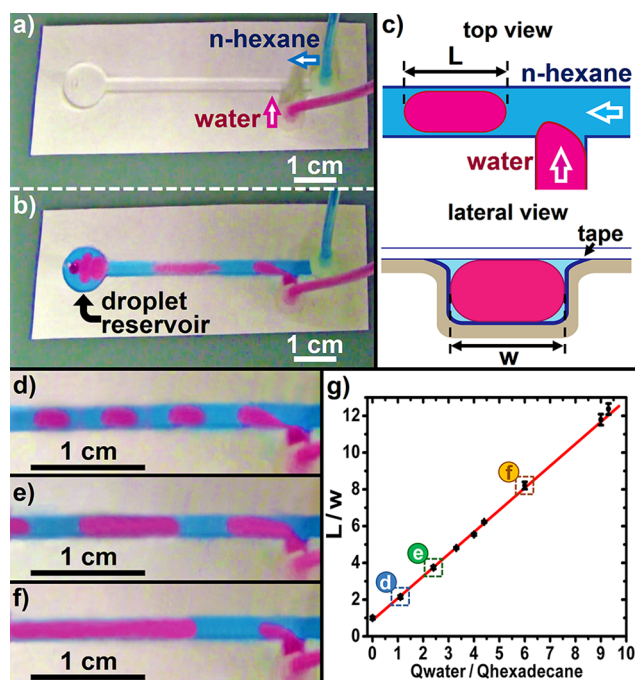


Figure 4. Droplet generator based on a “T”-shaped microfluidic device: (a) Embossed T-junction microfluidic device with the inlet tubes connected using PDMS slabs. (b) Droplet generator in use. (c) Schematic illustration of the geometry of the droplets inside the channel. (d–f) Droplet generator working at 9.5 Hz (d), 3.4 Hz (e), and 0.5 Hz (f). (g) Linear dependence on the flow rates of L/w in this system. Highlighted data correspond to the cases shown in panels d–f.

$\text{NH}_3(\text{g})$ through polyethylene tubes attached to the back of the device, the gases diffused through the bottom R^{F} paper layer in the channels containing the indicator solution. The gases dissolve in the solution flowing through the channel, change the pH of the solution, and are visualized by a color change in the indicator dyes (Figure 6d). The yellow–Phenol Red solution changes to purple under basic conditions, and the dark brown–Bromophenol Blue sodium salt solution changes to orange on exposure to acidic conditions. The high gas permeability of R^{F} paper provides a simple way to introduce a gas to a liquid (to capture components of the gas or as part of a sensor) without having a large exposed surface of liquid. The double-sided adhesive tape that is used to connect different paper layers prevents flow of gases from one channel to different channels in other layers. We allowed the delivery of gases to be targeted or localized by punching 3 mm i.d. holes on the double-sided adhesive tape, hence offering a guided low-resistance path to the desired channel.

Microfluidic Displays. After demonstrating a working gas-permeable 3D microfluidic device made by the cut-and-stack approach, we fabricated another microfluidic device with three letters “G”, “M”, and “W” connected via bottom channels following the cutting and stacking process described previously (Figures 5 and 6). Figure 7a–c shows such a channel in the process of being filled with a red aqueous solution while in Figure 7d a similar device-filled blue dye in hexadecane is shown demonstrating the omniphobicity of the paper channel. These devices have one inlet and one outlet on the top right part of “G” and “W”, respectively, as shown in Figure 7e. The inlet and outlet in these devices are located on the back of the device for convenience. We used Bromothymol Blue solution, a universal indicator (pH sensing range 6.0–7.6, displaying

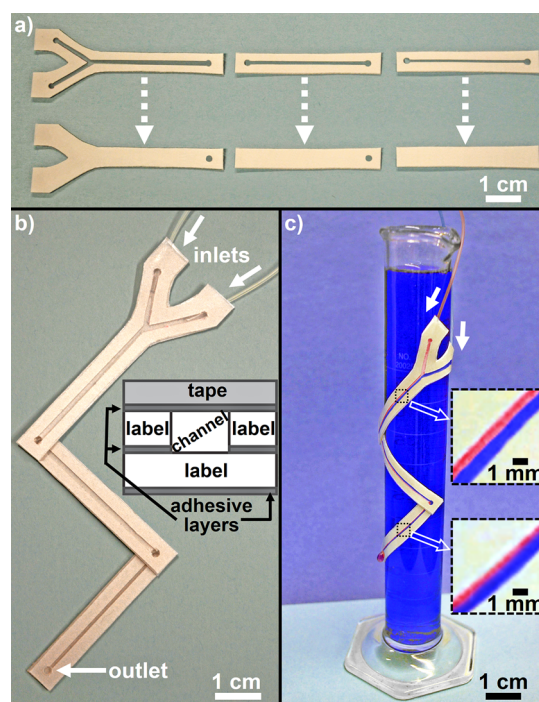


Figure 5. (a) Paper labels trimmed with a scalpel. The labels patterned with the outline of the channels (top) were stuck on top of the labels that will serve as the bottom of the channel, and the ensemble was silanized. (b) Paper device formed after sealing the channels by adhering a layer of transparent tape on top of the RF paper device (total thickness $\sim 600 \mu\text{m}$) and stuck the different sections of the device together using the back adhesive layer of the bottom paper label. The tubing connecting this device with a syringe pump can be secured by using the adhesive layer of the paper label at the top. This device admits to be reconfigured by changing the angle between its different sections. (c) Bendable microfluidic device conforming to the curved surface of a graduated cylinder containing an aqueous solution of Methylene Blue. This pressure-driven paper microfluidic device exhibits laminar flow when two miscible aqueous phases, each labeled with a different water-soluble dye (0.05% solutions of Methylene Blue or Congo Red in water), were pumped through a Y-junction at a flow rate of $100 \mu\text{L}/\text{min}$ (Reynolds number $Re = 80$).

yellow, green, and blue in acidic, neutral, and alkaline solutions, respectively), to demonstrate the possibility to induce sequential changes in the pH of a solution flowing through a microchannel made of R^{F} paper by taking advantage of the gas permeability of this paper device. The three letters displayed in Figure 7e were initially green with the solution flowing from “G” to “W” along the direction of the arrow. A vial containing a solution of 15% NH_4OH (NH_3 source) was connected to the back of the device via a 1/32” diameter Teflon tube. We inserted the end of the tube into a PDMS slab for support and attached the tube to the nonpatterned bottom layer of the device using a ring of double-sided adhesive tape. The $\text{NH}_3(\text{g})$ source was connected to the “M” on the back of the device (bottom left of “M”, as indicated by an arrow in Figure 7f), resulting in a colorimetric change of “M” and “W” from green to blue. The color of the letter “G” remained green, indicating that $\text{NH}_3(\text{g})$ did not diffuse into the letter “G” under fluid flow. After the exposure of “M” to $\text{NH}_3(\text{g})$, we exposed the letter “W” (arrow in Figure 7g) to $\text{HCl}(\text{g})$ coming through the bottom paper layer in an analogous way to what was done for $\text{NH}_3(\text{g})$. A vial containing concentrated HCl (fuming HCl) was used as our acidic gas source. The acidic gas, $\text{HCl}(\text{g})$,

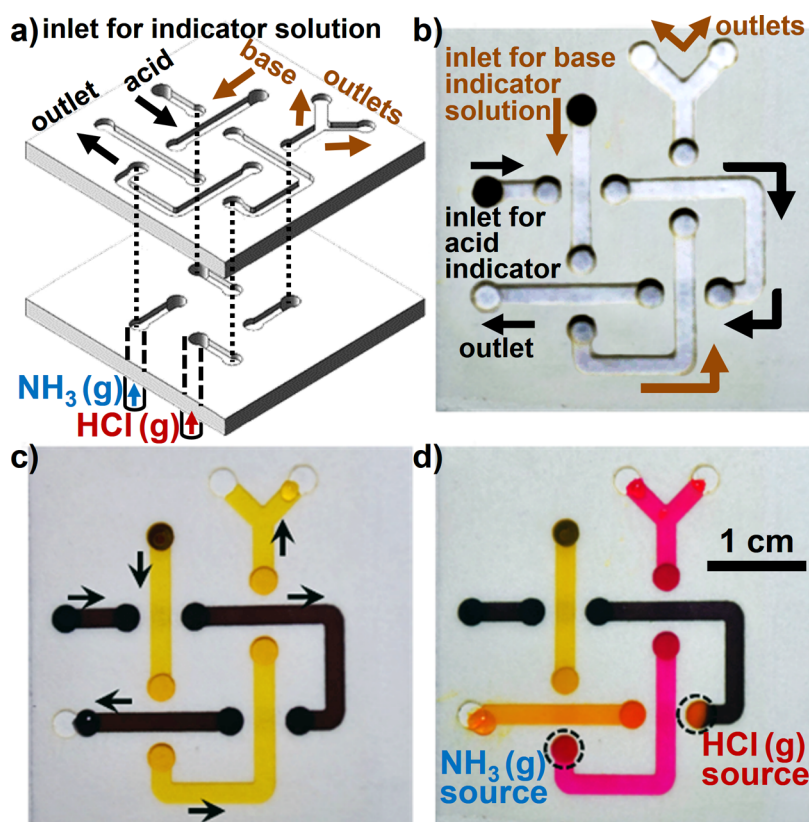


Figure 6. (a) Schematic illustration of a paper-based 3D microfluidic device fabricated by the cut-and-stack method—for more details, see Supporting Information Figure S8. The device allows multiple streams of fluid (acid and base) to cross each other without mixing. Gas sources are connected to the back of the channels; arrows indicate the directions of fluid and gas flow through the device. Note: the top layer of polymer tape and bottom layer of uncut paper are not shown to highlight the fluidic channels. (b) Photographs the 3D microfluidic device. Fluid inlets are connected to the underside of the device (indicated by a darker coloration in the channel). (c) Flowing phenol red (yellow) and bromophenol blue sodium salt (brown) pH-indicator solutions through the device channels. (d) The yellow indicator changes color to red when exposed to basic gas (NH_3) and the dark brown solution changes color to orange under acidic conditions. Gas inlets attachment locations are indicated by black dotted circles in (d).

neutralized the ammonium hydroxide present in the solution of indicator and split the fluid flowing through the “W” into two pH regions where the solution again turned yellow on the side of the microfluidic channel exposed to the acid while the other half remained blue (Figure 7g). We used this effect to demonstrate that the gas-permeability of a microchannel can be controlled by partially covering the width of the channel with a gas-impermeable layer, like tape, therefore limiting the ability for a gas to be introduced to the whole channel. A closer look at the inlet and outlet (Figure 7e,f) of each letter reveals a square dark spot in the background except for the inlet of letter “W” which has a triangular dark spot. These darkened spots are the channels that connect the letters except that for letter “W” the channel has been partially blocked with tape to allow gas diffusion to only occur through half of the channel (the unblocked triangle). When we attached the HCl inlet tube under this channel, only half of the channel changed color from blue to yellow. The acid (yellow) and basic (blue) solutions, as expected, did not mix under laminar flow. After the fluid flow was stopped, the yellow and blue solutions gradually mixed due to diffusion (Figure 7h).

96-Zone Plate. We fabricated 96-zone plates by mechanically embossing Whatman #5 chromatography paper between two ABS dies and rendering the surfaces omniphobic by silanization with $\text{R}^{\text{F}}\text{SiCl}_3$ (see Supporting Information Figure S2). Embossed wells with a diameter of 12 mm and a depth of

2 mm could hold aqueous solutions with a volume of up to 100 μL . We similarly fabricated multiwell plates of tunable depth and diameter through the cut-and-stack method. The depth of the well was controlled by the number of layers used to make the device (200 μm per sheet of paper), while the diameter of the wells was determined by the size of holes made on the paper (Supporting Information Figure S3).

CONCLUSIONS

A two-step process—embossing or cutting, treatment with perfluorinated $\text{R}^{\text{F}}\text{SiCl}_3$ as a vapor, followed by assembly—makes it possible to fabricate open channel microfluidic devices on paper rapidly. Dies for embossing were fabricated in ABS using a 3D printer; they could be used multiple times (over 1000) with no damage or degradation in performance. Fluid flow behavior in these paper-based microfluidic devices is similar to that observed in PDMS-based open channel devices. We observed laminar flow, droplet generation through shearing in a T-device, and 3D flow in a multilayer device made by placing different layers of embossed paper on top of each other and connected them using double-sided adhesive tape. By connecting different layers through the pre-cut hole and covering the top with a layer of transparent adhesive tape, we created 3D microfluidic devices in which fluids could pass one or another in different layers without mixing. In principle, the gas-permeable devices reported here can be applied to any

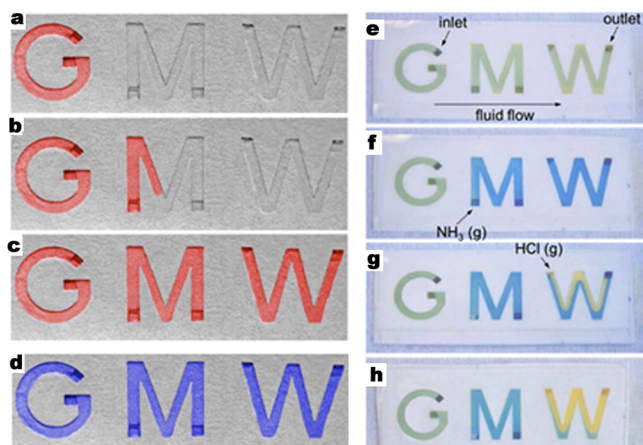


Figure 7. Cut-and-stack 3D microfluidic device with three letters (“G”, “M”, and “W”) making up the channels was made. (a–c) An aqueous red solution at different times in the channel filling process. (d) The same channel filled with a blue dye in hexadecane to demonstrate the omniphobicity of the paper channel. (e) A similar device with bromothymol blue solution only. The solution flowed from “G” to “W” with the inlet and outlet as indicated. (f) The starting point of “M” (where the arrow points to) was exposed to $\text{NH}_3(\text{g})$ from the back of the device. The color of “M” and “W” changed from green to blue. (g) The triangular part in “W” (indicated by the arrow) was exposed to $\text{HCl}(\text{g})$. The color of “W” changed partially from blue to yellow. (h) The solution was stopped and the yellow and blue solutions, as expected, diffused and mixed in “W” as expected.

liquid– or solid–gas physisorption process or chemical reaction with a broad range of applications in analysis, environmental monitoring, infochemistry, particle synthesis, and many others.

The cut-and-stack method is ideal for fabrication of reconfigurable 3D devices since the depth of the channels can be controlled by stacking layers of paper or using paper with different thicknesses. Adhesive and bendable microfluidic devices (as thin as $600\ \mu\text{m}$) were fabricated using paper labels and tape. Since paper can be folded, the cut-and-stack method can be combined with origami to build complex fluid transport systems or devices. Although embossing and the engraving techniques have their advantages, the versatility of the cut-and-stack method allows one to build more robust devices in a reliable manner using simple tools.

■ ASSOCIATED CONTENT

Supporting Information

More detailed details on the dimensions of the dies, additional devices, and videos of the running of experiments. This material is available free of charge via the Internet at <http://pubs.acs.org> or from the Web site of the Whitesides group (<http://gmwgroup.harvard.edu/pubs>).

■ AUTHOR INFORMATION

Corresponding Author

*(G.M.W.) Department of Chemistry and Chemical Biology, Harvard University, 12 Oxford Street, Cambridge, MA 02138, USA. E-mail: gwhitesides@gmwgroup.harvard.edu.

Present Address

#(X.L.) Department of Mechanical Engineering, McGill University, 817 Sherbrooke Street West, Montreal, Quebec, Canada H3A 0C3.

Author Contributions

△R.V.M. and M.M.T. contributed equally to this work.

Author Contributions

G.M.W., M.M.T., R.V.M., and X. L. conceptualized the project. M.M.T., R.V.M., X.L., and M.B.J.A. developed techniques for embossing. J.B., M.M.T., and R.V.M. imaged the devices. M.M.T., W.L., J.B., and R.V.M. developed the cut-and-stack methodology. R.V.M., M.M.T., and W.L. characterized the performance of the devices. G.M.W. advised and oversaw the research. All authors contributed to the writing of the manuscript. contributed equally to this work.

Notes

The authors declare no competing financial interest.

■ ACKNOWLEDGMENTS

This research was supported by the Bill and Melinda Gates Foundation under award 51308. M.M.T. acknowledges support from a Nanoscale Science and Engineering Centre fellowship at Harvard University and a subcontract from a Department of Energy (DESC0000989) award to Northwestern University for salary support. R.V.M. acknowledges funding by the FP7 People program under the project Marie Curie IOF-275148. J.B. acknowledges salary support from the Materials Research Science and Engineering Center under MRSEC award DMR-0820484. This work was performed in part using the facilities of the Center for Nanoscale Systems (CNS), a member of the National Nanotechnology Infrastructure Network (NNIN), which is supported by the National Science Foundation under NSF award PHY-0646094. CNS is part of the Faculty of Arts and Sciences at Harvard University.

■ REFERENCES

- (1) Chin, C. D.; Laksanasopin, T.; Cheung, Y. K.; Steinmiller, D.; Linder, V.; Parsa, H.; Wang, J.; Moore, H.; Rouse, R.; Umvilighozo, G. *Nat. Med.* **2011**, *17*, 1015–19.
- (2) Neethirajan, S.; Kobayashi, I.; Nakajima, M.; Wu, D.; Nandagopal, S.; Lin, F. *Lab Chip* **2011**, *11*, 1574–86.
- (3) Jokerst, J. C.; Emory, J. M.; Henry, C. S. *Analyst* **2012**, *137*, 24–34.
- (4) Ellerbee, A. K.; Phillips, S. T.; Siegel, A. C.; Mirica, K. A.; Martinez, A. W.; Striehl, P.; Jain, N.; Prentiss, M.; Whitesides, G. M. *Anal. Chem.* **2009**, *81*, 8447–52.
- (5) Martinez, A. W.; Phillips, S. T.; Whitesides, G. M.; Carrilho, E. *Anal. Chem.* **2009**, *82*, 3–10.
- (6) Nie, Z.; Nijhuis, C. A.; Gong, J.; Chen, X.; Kumachev, A.; Martinez, A. W.; Narovlyansky, M.; Whitesides, G. M. *Lab Chip* **2010**, *10*, 477–83.
- (7) Dungchai, W.; Chailapakul, O.; Henry, C. S. *Anal. Chem.* **2009**, *81*, 5821–26.
- (8) Mao, X.; Huang, T. J. *Lab Chip* **2012**, *12*, 1412–16.
- (9) Schilling, K. M.; Lepore, A. L.; Kurian, J. A.; Martinez, A. W. *Anal. Chem.* **2012**, *84*, 1579–85.
- (10) Carrilho, E.; Martinez, A. W.; Whitesides, G. M. *Anal. Chem.* **2009**, *81*, 7091–95.
- (11) Lu, Y.; Shi, W.; Jiang, L.; Qin, J.; Lin, B. *Electrophoresis* **2009**, *30*, 1497–500.
- (12) Bras, J.; Sadocco, P.; Belgacem, M. N.; Dufresne, A.; Thielemans, W. *Mater. Chem. Phys.* **2010**, *120*, 438–45.
- (13) Glavan, A. C.; Martinez, R. V.; Maxwell, E. J.; Subramaniam, A. B.; Nunes, R. M.; Soh, S.; Whitesides, G. M. *Lab Chip* **2013**, *13*, 2922–30.
- (14) Glavan, A. C.; Martinez, R. V.; Subramaniam, A. B.; Yoon, H. J.; Nunes, R.; Lange, H.; Thuo, M. M.; Whitesides, G. M. *Adv. Funct. Mater.* **2014**, *24*, 60–70.
- (15) Roper, M. G.; Shackman, J. G.; Dahlgren, G. M.; Kennedy, R. T. *Anal. Chem.* **2003**, *75*, 4711–17.
- (16) Plouffe, B. D.; Radisic, M.; Murthy, S. K. *Lab Chip* **2008**, *8*, 462–72.

- (17) Wu, Z.; Willing, B.; Bjerketorp, J.; Jansson, J. K.; Hjort, K. *Lab Chip* **2009**, *9*, 1193–99.
- (18) Zhu, Y.; Chen, H.; Du, G.-S.; Fang, Q. *Lab Chip* **2012**, *12*, 4350–54.
- (19) Li, L.; Ismagilov, R. F. *Biophysics* **2010**, *39*.
- (20) Xie, J.; Miao, Y.; Shih, J.; Tai, Y.-C.; Lee, T. D. *Anal. Chem.* **2005**, *77*, 6947–53.
- (21) Li, W.; Greener, J.; Voicu, D.; Kumacheva, E. *Lab Chip* **2009**, *9*, 2715–21.
- (22) Abate, A. R.; Kutsovsky, M.; Seiffert, S.; Windbergs, M.; Pinto, L. F.; Rotem, A.; Utada, A. S.; Weitz, D. A. *Adv. Mater.* **2011**, *23*, 1757–60.
- (23) Bhagat, A. A. S.; Hou, H. W.; Li, L. D.; Lim, C. T.; Han, J. *Lab Chip* **2011**, *11*, 1870–78.
- (24) Martinez, R. V.; Branch, J. L.; Fish, C. R.; Jin, L.; Shepherd, R. F.; Nunes, R.; Suo, Z.; Whitesides, G. M. *Adv. Mater.* **2013**, *25*, 205–12.
- (25) Novak, R.; Ranu, N.; Mathies, R. A. *Lab Chip* **2013**, *13*, 1468–71.
- (26) Kunnari, V.; Salminen, K.; Oksanen, A. *Pap. Puu—Pap. Timber* **2007**, *89*, 46–49.
- (27) Qin, D.; Xia, Y.; Whitesides, G. M. *Nat. Protoc.* **2010**, *5*, 491–502.
- (28) Hetsroni, G.; Mosyak, A.; Pogrebnyak, E.; Yarin, L. *Int. J. Heat Mass Transfer* **2005**, *48*, 1982–98.
- (29) Naher, S.; Orpen, D.; Brabazon, D.; Morshed, M. M. *Adv. Mater. Res.* **2010**, *83*, 931–39.
- (30) Leshansky, A.; Afkhami, S.; Jullien, M.-C.; Tabeling, P. *Phys. Rev. Lett.* **2012**, *108*, 264502.
- (31) Weaver, J. A.; Melin, J.; Stark, D.; Quake, S. R.; Horowitz, M. A. *Nat. Phys.* **2010**, *6*, 218–23.
- (32) Suh, Y. K.; Kang, S. *Micromachines* **2010**, *1*, 82–111.
- (33) Nisisako, T.; Torii, T.; Higuchi, T. *Lab Chip* **2002**, *2*, 24–26.
- (34) Garstecki, P.; Fuerstman, M. J.; Stone, H. A.; Whitesides, G. M. *Lab Chip* **2006**, *6*, 437–46.
- (35) Xu, J.; Li, S.; Tan, J.; Luo, G. *Microfluid. Nanofluid.* **2008**, *5*, 711–17.